Phys. Biol. **5** (2008) 036007 (8pp) doi:10.1088/1478-3975/5/3/036007

The nonlinear mechanical response of the red blood cell

Young-Zoon Yoon[1,2], Jurij Kotar[1], Gilwon Yoon[3] and Pietro Cicuta[1]

[1] Cavendish Laboratory and Nanoscience Center, University of Cambridge, Cambridge CB3 0HE, UK
[2] Department of Physics, Sungkyunkwan University, Suwon 440-746, Korea
[3] Institute for Biomedical Electronics, Seoul National University of Technology, Seoul 139-743, Korea

Received 30 May 2008
Accepted for publication 23 July 2008
Published 13 August 2008
Online at stacks.iop.org/PhysBio/5/036007

Abstract
We measure the dynamical mechanical properties of human red blood cells. A single cell response is measured with optical tweezers. We investigate both the stress relaxation following a fast deformation and the effect of varying the strain rate. We find a power-law decay of the stress as a function of time, down to a plateau stress, and a power-law increase of the cell's elasticity as a function of the strain rate. Interestingly, the exponents of these quantities violate the linear superposition principle, indicating a nonlinear response. We propose that this is due to the breaking of a fraction of the crosslinks during the deformation process. The soft glassy rheology model accounts for the relation between the exponents we observe experimentally. This picture is consistent with recent models of bond remodeling in the red blood cell's molecular structure. Our results imply that the blood cell's mechanical behavior depends critically on the deformation process.

1. Introduction

The human red blood cell (RBC) is a biological structure of relative simplicity: it lacks a nucleus and intramembrane organelles. Its components are well characterized [1–3], and they can be summarized as a bilayer membrane, coupled to a thin tenuous cytoskeleton of spectrin filaments via two complexes of few different proteins (ankyrin, band 3 and band 4.1). This outer membrane, held under tension by the cortical cytoskeleton, encloses a solution of dense hemoglobin. Despite its simplicity, the properties of this structure have puzzled researchers for decades. Investigations have focused on two related aspects of the physical structure: (1) explaining the biconcave discocyte shape that is found under physiological conditions (and a whole array of other morphologies that are found under perturbation or disease) and (2) measuring the mechanical properties of the cell and relating these to the structure. Regarding the shape, significant progress has been made recently showing how, by carefully balancing the membrane bending elasticity with tension from the underlying spectrin scaffold, the discocyte shape emerges as the equilibrium solution; the cup-shaped stomatocyte is the result of a perturbation that decreases the membrane area relative to the underlying skeleton [3]. On the issue of mechanical deformation, current experiments have mainly explored static deformations, despite the great importance of dynamical deformations for this cell. Large and transient deformations of the cell are involved in blood flow through thin capillaries [4, 5]. More generally, it is known that RBCs in suspension strongly affect the rheology of peripheral blood, with implications in several diseases [6]. The details of RBC mechanics have puzzled researchers for a long time, and complex rheological properties such as the existence of a threshold for plastic deformation and the presence of processes over very different timescales are already discussed in [5]. Historically, the RBC has variously been described as either a liquid or solid [7].

In this paper, we investigate the dynamical mechanical properties of the RBC by measuring its viscoelasticity over a range of environmental conditions. We focus on the deformation dynamics, looking at the correlation between the cell modulus and its shape, and on the effect of incubation leading to adenosine triphosphate (ATP) depletion. We relate the findings to phenomenological models for flow in kinetically arrested systems and to recent models describing the metabolic activity of the RBC, where the consumption of ATP controls the stiffness of the elastic network [8–10]. The normal biconcave human RBC has an approximately 25% more membrane surface area than the minimum required to enclose its volume, allowing deformations without an

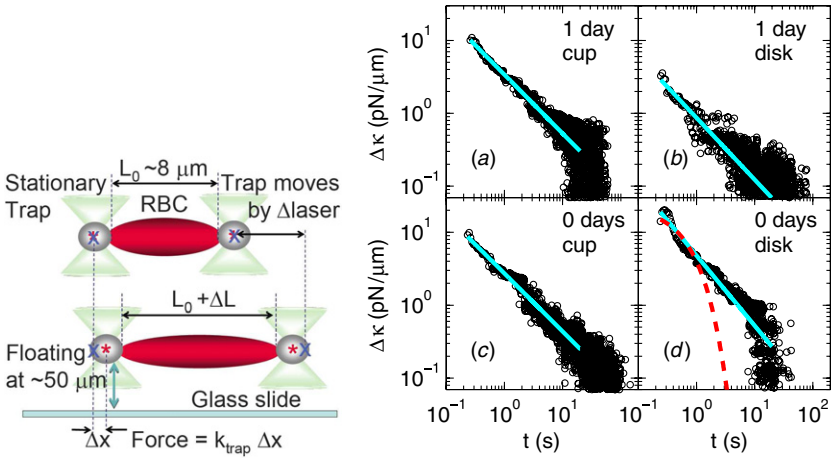

Figure 1. Diagram of the experimental setup. A cross marks the positions of the laser trap and a star marks the center of the bead, obtained via image analysis. (*a*)–(*d*) Decays of the measured time-dependent cell stiffness $\kappa(t)$ as a function of time. Solid lines are power-law fits described in the text; the dashed line in (*d*) is a single exponential fit to the data, showing very poor agreement. The plateau value has been subtracted from the data and from all the fits. The time-relaxation data show power-law decays with exponents $\simeq 3/4$.

extension of the membrane [11]. Therefore the mechanical response of the cell is related primarily to the bending and shear elastic moduli of its membrane, and to the viscosities of membrane and bulk. These quantities have been measured with various techniques, in particular micropipette aspiration [12], shape flickering [13–17], deformation in flow [16], electric fields [18] and optical tweezers [19–22]. Existing measurements give very different values. For example, independent experiments using micropipette aspiration yield a shear modulus of between 6 and 10 μN m^{-1} [12], and similar values are seen in shape relaxation following an external deformation [18]. Optical tweezer measurements also report a wide range of shear modulus, but the discrepancies between these results are in part the result of applying different geometrical models to extract the modulus from the measured forces: 2.5 ± 0.4 μN m^{-1} assuming a flat disc geometry [19], 200 μN m^{-1} assuming a spherical initial shape [20, 23], 11–18 μN m^{-1} comparing to a finite element simulation of the deformation [22]. A satisfactory analytical approximation for the geometry of a cell pulled by tweezers is still not available, and is not the topic of this work. We instead choose to report the directly measured mechanical properties, showing that even the model-independent dynamical stiffness of the cell is strongly dependent on the deformation protocol. Our key result is that the RBCs' response cannot be explained within the framework of linear viscoelasticity.

2. Experimental methods

Fresh blood was drawn from a healthy volunteer donor and diluted in phosphate-buffered saline (PBS) with acid citrate dextrose (Sigma C3821) and 1 mg ml^{-1} bovine serum albumin (BSA) (Sigma A4503) at pH 7.4. For studying the effect of aging time after drawing, cells were incubated with glucose-free PBS in a hot bath plate either at 37° C for 24 h with a 10^{-2} penicillin–streptomycin solution (GIBCO, Invitrogen 15070063) to prevent microbial growth, or at 4° C for 24 h. A control group was incubated with 100 mg dl^{-1} glucose in PBS buffer. These protocols provide samples that are a mixture of discocyte and stomatocyte cells, with an increasing fraction of discocytes after 1 day's incubation.

The optical tweezers' setup consists of a laser (IPG Photonics, PYL-1-1064-LP, $\lambda = 1064$ nm, $P_{\max} = 1.1$ W) focused through a water immersion objective (Zeiss, Achroplan IR 63×/0.90 W) trapping from below. The laser beam is steered via a pair of acousto-optic deflectors (AA Opto-Electronic, AA.DTS.XY-250@1064 nm) controlled by custom-built electronics allowing multiple trap generation with subnanometer position resolution. The trapping potential is locally described by a harmonic spring, and the trap stiffness was calibrated by measuring the thermal displacements of a trapped bead. The trapping stiffness at maximum power when trapping two beads (as in this work) is $k_{\text{trap}} = 44$ pN μm^{-1} on each bead. The sample is illuminated with a halogen lamp and is observed in a bright field with a fast complementary metal oxide semiconductor (CMOS) camera (Allied Vision Technologies, Marlin F-131B).

Carboxylated silica beads of 5.0 μm diameter (Bangs Labs) were washed in Mes buffer (Sigma M1317). They were then functionalized by resuspending in Mes buffer and incubating for 8 h at 37° C with Lectin (0.25 mg ml^{-1}) (Sigma L9640) and EDC (Sigma E1769) (4 mg ml^{-1}). This made them very sticky to the RBC, probably through binding to glicoproteins or sugars on the outer side of the RBC membrane. To prevent the RBCs from sticking on the glass surfaces of the chamber, BSA was coated on the slide glass. Using the tweezers, two beads are brought to an RBC and attached diametrically across a cell. This construct is then maintained floating well above the glass slide surface (at about ten times the bead diameter) to minimize any hydrodynamic drag from the solid surface. The cells are quite monodisperse in size, with an initial cell length (the diameter) $L_0 \sim 8\mu$m. The area of contact between the bead and the cell varies in the range 3–4.5 μm^2, and we find no correlation of the patch area with any of the experimental results. This arrangement is drawn in figure 1. During all the deformation protocols, one laser trap

is kept fixed at its initial position while the other trap is moved away by a distance Δlaser. We focus on tracking the bead in the immobile trap, measuring the difference Δx between the bead and the known laser position. Bead positions are obtained using a custom image analysis code written in Matlab. From the displacement Δx, the stretching force is calculated. The cell is elongated by a distance $\Delta L = \Delta\text{laser} - 2\Delta x$, and we define the strain as $\gamma = \Delta L/L_0$. The resolution of the bead position via image analysis on each frame is around 5 nm, which translates into ± 0.22 pN of force resolution. This is significantly less than the random fluctuations caused by thermal noise. The cell stretching is recorded at $\sim$60 frames per second, and having checked that we could not observe a variation between measurements done at room temperature and at 37° C, we report on measurements made at room temperature. Temperature is known from previous studies to have only a slight influence on the mechanics of RBCs [14, 24].

3. Results and discussion

3.1. Stress relaxation

We perform stress-relaxation experiments by moving just one trap (i.e. actively moving one bead) by $\Delta\text{laser} = 3.5$ μm at 20 μm s^{-1} and monitoring the force acting on the bead in the stationary trap. The force is observed to decay toward a plateau value, which (crudely speaking) is reached within less than half a minute. We define the time-dependent stiffness of the RBC to be $\kappa(t) = F(t)/\Delta L(t)$. The whole set of experiments is fitted very well by the following 3-parameter power-law function:

$$\kappa(t) = \kappa_\infty + \Delta\kappa(t) \doteq \kappa_\infty + \Delta\kappa_0 (t/t_0)^{-\alpha}, \qquad (1)$$

where we fix $t_0 = 1$ s to obtain a dimensionless time. We use the first 20 s of the decay to fit the values of κ_∞, $\Delta\kappa_0$ and α because in this range there is little noise in the data. It can be seen that the power-law decay holds for longer times as well. Our data extend to long enough times to clearly show that a single exponential fails to describe the data. In previous experiments of this type, the decay was observed only at short times, and a single exponential was used to fit the stress relaxation [19]. In [5], a single exponential decay, with a timescale of around 0.1 s was used to fit the shape relaxation, and it is apparent that the fit leads to very correlated residuals. In other work, a double exponential was used to fit shape relaxation data, obtaining a fast and a slow timescale of 0.1 and 0.9 s respectively [18]. If we fit an exponential to our data, we obtain a value for the relaxation timescale of $\tau \simeq 0.6$ s, but it needs to be stressed that this value has no real meaning and is simply the result of the time window chosen to fit the data. In figure 1(*d*), which are data for a fresh discocyte, we show that the single exponential fit is very poor indeed. Even a stretched exponential function, which describes in general relaxations with a discrete spectrum of relaxation times (4-parameters, not shown), gives a poor fit to the data. Whilst we have stressed that it is incorrect to assume that there is a timescale for relaxation in this system, we wish to clarify that over matching time windows our data are in agreement with published experiments such as those of [18, 19]. We therefore do not contradict in any way the value of the elastic shear modulus or the timescales obtained in those previous investigations, but rather make the point that they should be taken only as effective properties. In section 3.4 we return to the significance of the power-law decay, and how this is related to the physical origin of the cell's rheological behavior.

Figure 1 shows examples of the time relaxation of $\Delta\kappa(t)$ plotted separately for each of discocyte and cup-shaped stomatocyte cells, fresh and after 1 day of incubation. In all cases, the stiffness is fit over two decades in time by the form of equation (1). The power-law exponents are the same within experimental error; the mean of all the power-law exponents measured is $\alpha = 0.75 \pm 0.16$ for fresh cells and $\alpha = 0.82 \pm 0.09$ for cells incubated over 1 day. A total of 11 different cells were measured this way. These exponent values are very close to the dependence found recently for the shear dissipative modulus in [25] by magnetic bead cytometry (under very small deformations compared to this work), where the exponent is reported to be 0.64.

The value of the ratio $\Delta F_0/F_\infty$, i.e. the fraction of the stress that decays over time, also appears independent of the shape and cell age, and is between 0.55 and 0.75. At short times, i.e. 0.1 s after deformation, more than half of the time-dependent modulus is still not equilibrated. This is a very significant fraction of the response, i.e. much more than half of the stress decays over time. Physiological deformations occur with a timescale of approximately 1 s. Here at 1 s the response has already decayed by approximately one-third, but still in some cases only a little more than one-half of the response is elastic and the rest remains still time dependent. This illustrates the importance of understanding the cell dynamics.

The fact that the data are described so well by equation (1) implies that there are two components to the cell elastic modulus: a time-dependent and a long-time equilibrium modulus. Power-law relaxations are well known in systems near the gelation point and in entangled polymer solutions [26]; however, we anticipate here that we will discuss, how for the RBC, the form of equation (1) does not originate from polymer relaxation nor gel cluster dynamics.

3.2. Deformations varying the strain rate

To investigate further the dynamical modulus of the cell, we perform a triangle wave deformation experiment using speeds of 20, 5, 1 and 0.2 μm s^{-1}, and 3.5 μm laser trap displacement[4]. Figure 2(*a*) shows that the force measured over time is approximately proportional to the applied strain. The forces measured here are comparable to previous experiments [19]. The slight mismatch between the applied strain and the stress can be seen more clearly in figure 2(*b*) as a hysteresis loop. There is a slight difference between the onset of the first cycle and all the following ones. By observing many instances of this protocol, we believe that this is due to the cell

[4] For one speed and condition (data not shown), we looked for a dependence on the deformation amplitude by applying triangle waves of amplitudes 1, 5 and 7 μm and obtained the same stiffness as for 3.5 μm.

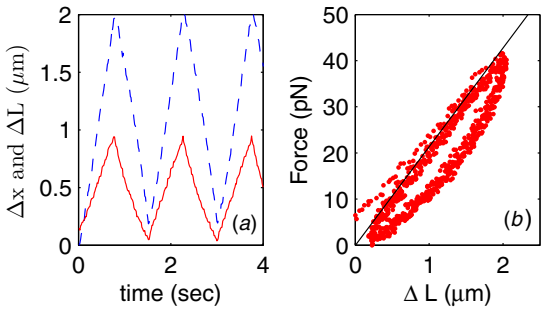

Figure 2. (*a*) The dashed line is the elongation ΔL of the RBC subject to a triangle wave trap displacement and the solid line is Δx of the bead in the stationary trap. (*b*) Force versus elongation of the cell ΔL, for the same data as in panel (*a*). The solid line is a linear fit to the force during extension; the area inside the hysteresis loop is the energy dissipated per cycle.

rearranging its position precisely along the axis of the strain experiment. It is clear from this figure that there is no further evolution of the stress–strain curves over the run, which last typically tens of cycles. The cell's response is predominantly elastic, and the gradient of the force versus elongation data as in figure 2(*b*), taken over the extension, gives the stiffness κ of the cell. This stiffness is an effective property of the cell, and may be a valid modulus for describing the cell's response in physiological processes such as elongating to squeeze through thin capillaries. The experimental speed of deformation can be converted into an approximate strain rate $\dot{\gamma}$ by dividing the bead velocity by the initial cell length (L_0). The cell stiffness is plotted in figure 3 against the strain rate. Our results show that there can be a large (factor of 3) difference between the stiffnesses in the dynamic range studied here, from 10^{-2} to 1 s^{-1}. This suggests that static stiffness, as measured for example by a micropipette, may not give the correct results for the physiological range of strain rates in circulation, which may involve deformations of 10% occurring every second, i.e. strain rates of the order of 0.1 s^{-1}.

The cell stiffness is related to the strain rate through the function

$$\kappa(\dot{\gamma}) - \kappa_0 \sim \dot{\gamma}^{\beta}, \tag{2}$$

with $\beta \simeq \frac{1}{4}$.

The uniaxial extension in our experiments is similar to the uniaxial deformation induced by an optical stretcher, studied in [21]. In that work the cell membrane was approximated geometrically as a thin spherical shell, and a relation was derived linking the elongation of the cell to the applied stress and Young's modulus E. Assuming that the cell has radius ρ and that the bead is attached to the cell over an area of radius ρ_{patch}, this relation is

$$\Delta L = F \frac{\rho^2}{\pi \rho_{\text{patch}}^2} \frac{1}{Eh}, \tag{3}$$

where h is the thickness of the whole membrane which is of the order of $h \simeq 40$ nm. Taking $\rho \simeq 4\mu$m and the patch radius to be of the order of 2μm, this relation enables the values

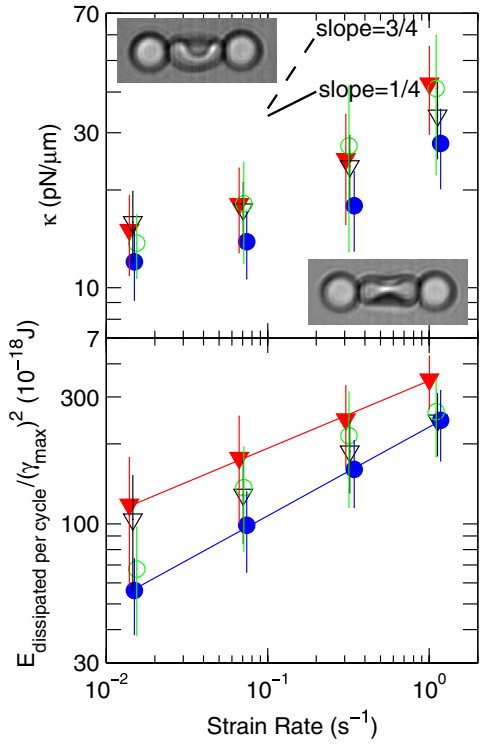

Figure 3. Strain rate dependence of the RBC stiffness κ and the energy dissipation. Markers indicate the different conditions studied here: (▼) fresh-discotic, (▽) fresh-stomatocyte, (●) 1 day-discotic, (○) 1 day-stomatocyte.

for the stiffness to be turned into Young's and shear modulus $G = E/3$ for a Poisson ratio of 0.5:

$$\kappa \simeq Eh = 3Gh. \tag{4}$$

The shear modulus values obtained in this way are Gh between 3 and 6×10^{-6} N m^{-1}, which are in agreement with [12, 19, 21, 22]. These measurements of the shear modulus are very approximate due to the approximations involved in obtaining relations, such as in equation (3). For this reason the data in this paper are presented as a raw stiffness, which is not subject to approximations. However, these considerations are useful to clarify that the main contribution to the measured stiffness comes from the membrane's shear modulus. Bending and stretching are negligible for this deformation.

The hysteresis in the stress–strain curves is a measure of energy dissipation in the cell, and is shown in figure 3. In order to compare the results from different strain amplitudes, the dissipated energy is presented as the work per cycle, normalized by the square of the strain amplitude γ_{max}. The dissipated energy follows a power law as a function of the strain rate, with an exponent that we assume is the same β as in equation (2). In all the cells, the strain rate dependence is well below the linear relation expected for a purely viscous system. The exponents fitted here are $\beta = 0.25$ for fresh discocytes and $\beta = 0.33$ for discocytes after 1 day's incubation. These values have higher precision than the stress-relaxation exponents because the triangle wave cycle is repeated many times.

3.3. Origin of energy dissipation

The dissipated energy per cycle in our experiments is of the order of 4–12 $\times$ 10^{-18} J. To understand the origin of the dissipation, it is important to consider various possible sources. We first discuss the following three possibilities which can be ruled out as the main source of dissipation in our experiments. (1) Dissipation can arise from the phospholipid bilayer itself. Its viscosity is around 0.3 Pa s [27]. Considering a simplified geometry of deformation of two flat plates, the dissipated energy from the bilayer is around 0.6 $\times$ 10^{-18} J per cycle at $\dot{\gamma} = 10^{-2}$ s^{-1}. This is an order of magnitude below our results but, since this 'Newtonian liquid' contribution to the dissipation grows linearly with the strain rate it would eventually dominate the response at higher deformation rates. (2) Dissipation can arise from the drag of anchoring proteins through the bilayer. The number of bonds in the spectrin mesh has been estimated to be around 35 000 [28]; so a number of anchoring sites similar to the phospholipid bilayer can be assumed. The drag arising from the motion of these sites as they are dragged through the bilayer can be estimated using the drag coefficient valid for objects of the order of a few nanometers [29]. Assuming a 10% strain of the mesh elements (length 200 nm) at a frequency between 10^{-2} and 1 s^{-1}, 2 nm as the anchor radius and the bilayer viscosity quoted above, this gives dissipation of between 3 $\times$ 10^{-27} J and 3 $\times$ 10^{-25} J per anchor group per cycle, i.e. a total of between 10^{-21} J and 10^{-19} J for the whole cell. (3) Bulk hemoglobin has a viscosity of around 46 Pa s [30]; therefore by again approximating the problem by considering the cell as parallel plates of area L_0^2, being strained by γ at a strain rate $\dot{\gamma}$, we obtain dissipation per cycle in the range 2 $\times$ 10^{-20}–2 $\times$ 10^{-18} J for our experimental conditions[5]. This rules out the dissipation due to shearing of the interior of the cell as the source of the observed dissipation. Having considered these three sources of dissipation, and finding them to be a few orders of magnitude below the experimentally observed values, we are left to consider the membrane cytoskeleton (whether passively or actively) as the source of dissipation. In previous work, it had been seen that the viscosity of the phospholipid bilayer was insufficient to explain the observed relaxation times for the cell shape driven by the experimentally measured elastic shear modulus. It was suggested [18] that the viscoelasticity of the cell was determined by the parts of the cytoskeleton coupled to the membrane. In this work we agree with this conclusion, but we point out that the three sources of dissipation considered in this section, aside from being negligible, also cannot explain the nonlinearity of the response. We therefore concentrate on a nonlinear model which can account for our data, keeping in mind that the cytoskeleton is the element likely to dominate the cell mechanics. In [5], the restructuring of the cytoskeleton was mentioned as the mechanism underlying the very slow (tens of minutes) creep response of RBCs.

[5] In the work of [30] the cytoplasmic and solution viscosities were compared directly using vibrational echo experiments, and were found to be the same. These measurements clarified a long-standing issue of a possible much larger viscosity inside the cell; see, for example, the discussion in [16].

3.4. Nonlinear rheology and modeling with soft glassy rheology

In linear viscoelasticity, the dependence of the modulus on the strain rate is related to the form of the stress relaxation via a modified Laplace transform [26]. In the case of a power-law decay with $\kappa(t) - \kappa_\infty \sim t^{-\alpha}$, we expect $\kappa(\dot{\gamma}) - \kappa_0 \sim \dot{\gamma}^\alpha$. This is very clearly not the case in the data of the present experiments, in which the exponent β is much smaller than α. This points to the fact that even though our strain amplitudes are not very large, only of the order of 20%, our experiment is in a nonlinear regime. The experimental finding can be understood as follows: the power-law relaxation is the manifestation of a system where at least a fraction of the bonds can break under stress and quickly reform, essentially remodeling the skeleton's network. There is an analogy between this molecular-scale picture and the more general situation of the rheology of a system where the components have to overcome potential barriers in order to flow. This condition is addressed by the soft glassy rheology (SGR) model which, assuming a distribution of energy wells of different depths, provides a framework for calculating the nonlinear response of the system [31]. The SGR model contains one principal parameter, x, which is the ratio of the available energy to the mean well depth. For $x < 1$, the model is in a glassy phase. The shear modulus is predicted to decay with time as $G \sim t^{-x}$, and the stress under the constant strain rate is $\sigma - \sigma_y \sim \dot{\gamma}^{1-x}$. The RBC power laws and exponents appear to be well described by the SGR model with a value of $x \simeq 3/4$.

The SGR model has been used previously to discuss cell mechanics. For example, Trepat *et al* in [32] reviewed the model, arguing about its importance in cell mechanics, and used it to describe the mechanics of muscle cells. In complex cells, which include a bulk cytoskeleton of various types of actively growing filaments, crosslinked and actuated by molecular motors, it is difficult to pinpoint the structural elements involved in giving an SGR type of response. However the situation in the RBC is much simpler, and we can speculate on the physical process which underlies the SGR model phenomenology that we observe. In the RBC, it is possible that the potential barriers to be overcome are the energies for releasing a spectrin filament from a crosslink. The filament would then re-bond in a configuration of lower stress. The presence of a long-lived residual stress in the stress relaxation implies the presence of either a fraction of permanent bonds or of a kinetically arrested state with residual stress, in both cases leading to a deviation from a purely power-law scaling at low strain rates which is visible in the stiffness data of figure 3. Computer simulations of the statical properties of a network that mimics the RBC cytoskeleton and has restructuring properties have been carried out in [33], but we are not aware of simulations that extend to the study of a dynamical response.

In the absence of external stresses it is known that ATP is required to open the spectrin–actin linker, whose bond energy is around 7 $k_B T$, i.e. 3 $\times$ 10^{-20} J [34, 35]. Using again the estimate of 35 000 linkers, this gives an energy of 10^{-15} J for opening all the linkers. Given that the dissipated energy

per cycle is between 4 and 12 $\times$ 10^{-18} J, this implies that either (a) only a small fraction of the bonds, around 1%, is broken during a cycle, (b) the bond energies under stress are reduced considerably, or (c) ATP and not solely mechanical energy is being used to break the bonds. Of these possibilities, the agreement with the soft glassy rheology observed here suggests a combination of (a) and (b), i.e. remodeling of the linkers under stress does not involve the full cost of breaking the spectrin–actin linker. The role of force in reducing the dissociation energy between spectrin linkers was discussed in [36]. The picture of a cytoskeleton proposed here that partially breaks and rearranges under tension is a possible and, in our view, a likely interpretation of why the SGR model is successful for the RBC, but we must stress that from our experiments there is no direct evidence for molecular-scale processes.

The dependence of the cell modulus on the strain rate measured in this work can also be compared to recent data obtained by monitoring the deformation induced via magnetic twisting cytometry (MTC). This is essentially a creep experiment performed on a pivoting magnetic bead bound to the outside of a RBC [25]. In MTC there is almost certainly a large influence of the membrane-bending elasticity, and the elastic component of the response in the data of [25] is dominated by a source of elasticity that is not found in our measurements with optical tweezers, most likely membrane curvature.

In the context of the SGR model, a system in the glassy phase will slowly 'age', falling into the deeper minima in the free energy landscape. A strongly imposed deformation applied in the glassy phase can then bring back the system to a configuration with a random distribution of energy wells. In an aged glassy system a large strain can therefore bring about a reduction in the mechanical modulus, an effect known as 'fluidization'. This has been reported very clearly in experiments on cells [32] and also for colloidal glasses [37]. In simulations of networks with bonds that can fail [33], fluidization is taken as a state with lower modulus that occurs after large strain; it is unclear if this is the same SGR phenomenology. We have performed experiments by keeping cells strained for several minutes and then relaxing to natural length. Within error, the mechanics is found to be the same as a cell that has not been stretched. We therefore do not find evidence of fluidization in our experiments, which could indicate that the distribution of energy minima in this system is rather narrow. This would also be consistent with the absence of significant aging in this system, compared to experiments on colloidal glasses [37].

3.5. ATP concentration

While the features of the dynamical response of all the cells are the same, we observe differences in the magnitude of the response depending on the shape of cell and the incubation protocol. The strongest influence, leading to a decrease of the cell modulus by almost a factor of 2 after 1 day of incubation, is the time from when the cells are drawn. Secondary to this effect of incubation time, we observe a correlation between the stiffness of the cell and its shape. The cup-shaped stomatocytes are almost twice as stiff as the discotic cells. The models recently proposed describe the active remodeling of the RBC's cytoskeletal network [35, 10]. ATP is expected to be strongly related to this activity, at least under the absence of an external force [10]. It is of interest that flickering of RBC ghost membranes at low frequencies was shown to depend on the intracellular MgATP [38], and the flickering has also been shown to decrease with cell aging [14]. Through the 1 day incubation protocol the ATP concentration inside the cell is depleted, and according to these references this would lead to stiffer cells. In contrast, in recent work, the ATP concentration was found not to play a role in the fluctuation spectrum of the cell [17]. Our results showing softening seem to imply an opposite effect, one possibility for this being that under reduction of ATP the cell loses some of its ability to reform the bonds that break under deformation. We find no appreciable difference between the cells incubated in the absence of glucose and in physiological glucose concentrations (data not shown). It is quite likely that the fluctuation spectrum, which corresponds to very small deformations close to the equilibrium shape, does not probe the same physical nonlinear process as larger scale deformations. The role of ATP would be important in those deformations that require dissociation of cytoskeletal or anchoring elements.

4. Outlook and conclusion

Our time-relaxation data confirm that the dynamics in the RBC, as also pointed out recently by Suresh and collaborators [25], is intrinsically free of a characteristic timescale. Our findings here are in contrast to many previous investigations of the RBC [18, 19, 22, 39], where limited datasets led to simplistic conclusions regarding the dynamics.

Our main experimental contributions are (1) the study of the cell modulus at varying strain rates, showing a large (factor of 3) increase in the cell stiffness as the cell is deformed at higher strain rates, (2) the measurement of energy dissipation as cells are deformed, (3) the comparison of constant strain rate measurements with stress-relaxation measurements. Together, these data have allowed us to show that the mechanics is not linear, and therefore depends on the deformation protocol, even for small deformations. The experiments reported here are well described by the soft glassy rheology (SGR) model, which predicts exactly the relation between the constant strain and stress-relaxation data observed. The soft glassy rheology framework is the only model we know that correctly predicts the very non-trivial relation between the power-law exponents in stress relaxation and as a function of the strain rate. This is the first investigation where this relation is tested by doing both experiments on the same system. It is interesting to find this complex behavior on such a simple structure as the RBC, as this may lead to a better understanding of the origin of SGR in other cell types.

As far as the dynamics in erythrocytes is concerned, there remains a range of strains to be explored to bridge between the infinitesimal deformations seen in spontaneous fluctuations [17] and the small deformations of magnetic bead cytometry

[25], up to the larger deformations explored in this work. It is possible that the nonlinearities described here might not be present at much smaller strains. With our current experimental setup and protocols it is not possible to perform 'active' pulling of the cells at displacements comparable to spontaneous fluctuations, where one might indeed expect to recover linearity. This is because at very small amplitudes, the beads spend most of the time at almost negligible force induced by the cell. This can lead to complications in the cell/bead coupling, since the cell has much more freedom to move than in our experiments. As mentioned, we did test 1 μm trap movements, as well as larger displacements, but we cannot bridge down to the level of fluctuations. The question of whether a linear regime exists at all for soft glassy materials is a very active one [31]. Within the framework of the soft glassy rheology model, which we find to hold very well for the RBC experiments, there could be no truly linear region for any value of external stress, however small. In other words, an external force would modify the state of the system in a way that is irreversible under thermal forces.

A final point of outlook relates to the area of synthetic systems that model and mimic cells. The RBC, being one of the simplest cell types, is an obvious model. A currently widely used model system is the unilamellar giant vesicle (GUV), which is a closed membrane bilayer of a size similar to the RBC [40]. It is possible to perform the same elongation experiments on GUVs, but unfortunately they do not help with comparison to the RBC, because even when large unilamellar vesicles are produced with an excess area, they are still quasi-spherical in shape, and as they are deformed by the tweezers they become taught at very small strains. However, there is a significant current activity in making GUVs with coupled synthetic cytoskeletons. By tuning the bilayer/cytoskeleton moduli to a similar ratio as in the RBC it should be possible to recreate the discotic shape with a large excess area, and it will be very interesting to study these systems under deformation.

Acknowledgments

We acknowledge funding by the Oppenheimer Fund, EPSRC, the Korea Foundation for International Cooperation of Science & Technology (KICOS) through grant 2007-00338 provided by the Korean Ministry of Science and Technology (MOST). We thank V Lew, I Poberaj, N Gov, E M Terentjev, J Guck, J Sleep, J Evans, W Gratzer and P G Petrov for advice and help.

Glossary

Optical tweezers. A micromanipulation technique based on a focused laser beam. As a result of transfer of the photons' momentum, the beam can exert a force on objects that have a different refractive index to their surrounding. They are widely used to trap and manipulate cells and colloidal particles.

Viscoelasticity. The mechanical response following a deformation in simple materials is either purely elastic or purely viscous. In contrast, biological materials are very often 'complex liquids', exhibiting elastic and viscous properties at the same time. This type of response is called viscoelasticity.

Erythrocyte. Red blood cell (RBC). It is not a cell in the usual eukaryotic sense, as it cannot reproduce. In mammals it has no nucleus, and has a particularly simple and easily deformable structure that makes it appealing as a model system to study cell mechanics.

Nonlinear response. Any deformation can be broken down into a set of infinitesimal deformations. A mechanical response is nonlinear when it is not true that the observed response to a deformation is a straightforward integral of the responses that correspond to the infinitesimal deformations.

Soft glassy rheology model. Also known as SGR, this is a model which describes several features of cell mechanics. It was originally developed in the context of packed colloidal systems (pastes), where particles lose the freedom to rearrange under thermal forces, but may still flow under the action of an external force. The model predicts power-law force relaxations as a function of time and power-law dependences on the frequency of deformation. The observed response is a function of a single parameter which is the ratio of the available energy to the average depth of the free energy landscape.

References

[1] Alberts B, Bray D, Lewis J, Raff M, Roberts K and Watson J D 1994 *Molecular Biology of the Cell* (New York: Garland Publishing)
[2] Boal D 2002 *Mechanics of the Cell* (Cambridge: Cambridge University Press)
[3] Lim G H W, Wortis M and Mukhopadhyay R 2002 Stomatocyte-discocyte–echinocyte sequence of the human red blood cell: evidence for the bilayer-couple hypothesis from membrane mechanics *Proc. Natl Acad. Sci.* **99** 16766
[4] Fischer T M, Stohr-Lissen M and Schmid-Schonbein H 1978 The red cell as a fluid droplet: tank tread-like motion of the human erythrocyte membrane in shear flow *Science* **202** 894
[5] Evans E A 1989 Structure and deformation properties of red blood cells: concepts and quantitative methods *Methods Enzymol.* **173** 3
[6] Suresh S 2006 Mechanical response of human red blood cells in health and disease: some structure-property-function relationships *J. Mater. Res.* **21** 1871
[7] Hochmuth R M 1982 Solid and liquid behavior of red cell membrane *Annu. Rev. Biophys. Bioeng.* **11** 43
[8] Tuvia S, Levin S V and Korenstein R 1992 Oxygenation-deoxygenation cycle of erythrocytes modulates submicron cell membrane fluctuations *Biophys. J.* **63** 599
[9] Tuvia S, Levin S, Bitler A and Korenstein R 1999 Mechanical fluctuation of the membrane-skeleton are dependent on f-actin ATPase in human erythrocytes *Biophys J.* **141** 1151
[10] Gov N S 2007 Active elastic network: cytoskeleton of the red blood cell *Phys. Rev.* E **75** 011921
[11] Jay A W L 1975 Geometry of the human erythrocyte: I. Effect of albumin on cell geometry *Biophys. J.* **15** 205

[12] Waugh R and Evans E A 1976 Viscoelastic properties of erythrocyte membranes of different vertebrate animals *Microvasc. Res.* **12** 291
[13] Brochard F and Lennon J F 1975 Frequency spectrum of the flicker phenomenon in erythrocytes *J. Phys. (France)* **36** 1035
[14] Fricke K and Sackmann E 1984 Variation of frequency spectrum of the erythrocyte flickering caused by aging, osmolarity, temperature and pathological changes *Biochim. Biophys. Acta* **803** 145
[15] Peterson S H S E M A 1992 Theoretical and phase contrast microscopic eigenmode analysis of erythrocyte flicker amplitudes *J. Phys. II (France)* **2** 1273
[16] Peterson M A, Strey H and Sackmann E 1992 Linear response of the human erythrocyte to mechanical stress *Phys. Rev.* A **45** 4116
[17] Evans J, Gratzer W, Mohandas N, Parker K and Sleep J 2008 Fluctuations of the red blood cell membrane: relation to mechanical properties and lack of atp dependence *Biophys J.* **94** 4134
[18] Engelhardt H, Gaub H and Sackmann E 1984 Viscoelastic properties of erythrocyte membranes in high-frequency electric fields *Nature* **307** 378
[19] Hénon S, Lenormand G, Richert A and Gallet F 1999 A new determination of the shear modulus of the human erythrocyte membrane using optical tweezers *Biophys J.* **76** 1145
[20] Sleep J, Wilson D, Simmons R and Gratzer W 1999 Elasticity of the red cell membrane and its relation to hemolytic disorders: an optical tweezers study *Biophys J.* **77** 3085
[21] Guck J, Ananthakrishnan R, Mahmood H, Moon T J, Cunningham C C and Käs J 2001 The optical stretcher: a novel laser tool to micromanipulate cells *Biophys. J.* **81** 767–84
[22] Dao M, Lim C T and Suresh S 2003 Mechanics of the human red blood cell deformed by optical tweezers *J. Mech. Phys. Solids* **51** 2259
[23] Parker K H and Winlove C 1999 The deformation of spherical vesicles with permeable, constant-area membranes: application to the red blood cell *Biophys J.* **77** 3096
[24] Artmann G M 1995 Microscopic photometric quantification of stiffness and relaxation time of red blood cells in a flow chamber *Biorheology* **32** 553
[25] Puig-de Morales-Marinkovic M, Turner K T, Butler J P, Fredberg J J and Suresh S 2007 Viscoelasticity of the human red blood cell *Am. J. Cell Physiol.* **293** 597
[26] Larson R G 1999 *The Structure and Rheology of Complex Fluids* (New York: Oxford University Press)
[27] Cicuta P, Keller S L and Veatch S L 2007 Diffusion of liquid domains in lipid bilayer membranes *J. Phys. Chem.* B **111** 3328
[28] Byers T J and Branton D 1985 Visualization of the protein associations in the erythrocyte membrane skeleton *Proc. Natl Acad. Sci.* **82** 6153
[29] Gambin Y, Lopez-Esparza R, Reffay M, Sierecki E, Gov N S, Genest M, Hodges R S and Urbach W 2006 Lateral mobility of proteins in liquid membranes revisited *Proc. Natl Acad. Sci.* **103** 2098
[30] McClain B L, Finkelstein I J and Fayer M D 2004 Vibrational echo experiments on red blood cells: comparison of the dynamics of cytoplasmic and aqueous hemoglobin *Chem. Phys. Lett.* **392** 324
[31] Sollich P, Lequeux F, Hébraud P and Cates M E 1997 Rheology of soft glassy materials *Phys. Rev. Lett.* **78** 2020
[32] Trepat X, Deng L, An S, Navajas D, Tschumperlin D, Gerthoffer W, Butler J and Fredberg J 2007 Universal physical response to stretch in the living cell *Nature* **447** 592
[33] Li J, Lykotrafitis G, Dao M and Suresh S 2007 Cytoskeletal dynamics of human erythrocyte *Proc. Natl Acad. Sci.* **104** 4937
[34] Bennett V 1989 The spectrin-actin junction of erythrocyte-membrane skeletons *Biochim. Biophys. Acta* **988** 107
[35] Gov N S and Safran S A 2005 Red blood cell membrane fluctuations and shape controlled by ATP-induced cytoskeletal defects *Biophys. J.* **88** 1859
[36] Lee J C-M and Discher D E 2001 Deformation-enhanced fluctuations in the red cell skeleton with theoretical relations to elasticity, connectivity, and spectrin unfolding *Biophys. J.* **81** 3178
[37] Viasnoff V and Lequeux F 2002 Rejuvenation and overaging in a colloidal glass under shear *Phys. Rev. Lett.* **89** 065701
[38] Levin S V and Korenstein R 1991 Membrane fluctuations in erythrocytes are linked to MgATP-dependent dynamic assembly of the membrane skeleton *Biophys. J.* **60** 733
[39] Hochmuth R M, Worthy P R and Evans E A 1979 Red cell extensional recovery and the determination of membrane viscosity *Biophys. J.* **26** 101
[40] Miao L, Seifert U, Wortis M and Döbereiner H-G 1994 Budding transitions of fluid-bilayer vesicles—the effect of area-difference elasticity *Phys. Rev.* E **49** 5389